Received: 19 June 2021 | Revised: 27 September 2021 | Accepted: 7 October 2021

DOI: 10.1049/qtc2.12026

IET Quantum Communication

The Institution of Engineering and Technology WILEY

ORIGINAL RESEARCH PAPER

Retrieval of exudate-affected retinal image patches using Siamese quantum classical neural network

Mahua Nandy Pal[1] | **Minakshi Banerjee**[2] | **Ankit Sarkar**[3]

[1]Department of Computer Science and Engineering, MCKV Institute of Engineering, Howrah, India

[2]Department of Computer Science and Engineering, RCC Institute of Information Technology, Kolkata, India

[3]TATA Consultancy Services Ltd, Hyderabad, India

Correspondence

Mahua Nandy Pal, Department of Computer Science and Engineering, MCKV Institute of Engineering, 243, GT Road (N), Liluah, Howrah-711204, West Bengal, India.
Email: mahua.nandy@gmail.com

Abstract

Deep neural networks were previously used in the arena of image retrieval. Siamese network architecture is also used for image similarity comparison. Recently, the application of quantum computing in different fields has gained research interest. Researchers are keen to explore the prospect of quantum circuit implementation in terms of supervised learning, resource utilization, and energy-efficient reversible computing. In this study, the authors propose an application of quantum circuit in Siamese architecture and explored its efficiency in the field of exudate-affected retinal image patch retrieval. Quantum computing applied within Siamese network architecture may be effective for image patch characteristic comparison and retrieval work. Although there is a restriction of managing high-dimensional inner product space, the circuit with a limited number of qubits represents exudate-affected retinal image patches and retrieves similar patches from the patch database. Parameterized quantum circuit (PQC) is implemented using a quantum machine learning library on Google Cirq framework. PQC model is composed of classical pre/post-processing and parameterized quantum circuit. System efficiency is evaluated with the most widely used retrieval evaluation metrics: mean average precision (MAP) and mean reciprocal rank (MRR). The system achieved an encouraging and promising result of 98.1336% MAP and 100% MRR. Image pixels are implicitly converted to rectangular grid qubits in this experiment. The experimentation was further extended to IBM Qiskit framework also. In Qiskit, individual pixels are explicitly encoded using novel enhanced quantum representation (NEQR) image encoding algorithm. The probability distributions of both query and database patches are compared through Jeffreys distance to retrieve similar patches.

KEYWORDS

cirq, qiskit, quantum circuit, retinal image patch retrieval, siamese network

1 | INTRODUCTION

Retina is the photoreceptor tissue at the back of the eye responsible for changing light into nerve impulse that is sent to the brain. Both ocular and circulatory diseases manifest symptoms at an early stage in retinal fundus images. One of the disease symptoms prevalent in the retina is the presence of exudate. Retinal damage is irreversible in nature. Early detection and timely treatment are essential to avoid blindness. Retinal fundus image retrieval technique can be used for computer-aided diagnosis of retinal and cardiovascular abnormalities. Content-based retinal patch retrieval process makes use of image characteristic features to retrieve similar patches, index-wise, from a database of affected and unaffected image patches with nominal human involvement. A consistent and rapid affected sample retrieval method will be of great help in improving the retinal screening process at an early disease stage.

Retrieval of affected fundus images is previously accomplished with the application of deep neural networks in this

domain. Siamese network is a class of network architecture, used for image similarity comparison. Siamese means twins. Siamese network is composed of two same neural networks, both having the same parameters. When two images from the same class are fed to these networks in parallel, they produce similar intermediate feature representations. Thus the difference between these two representations is lower when compared with the difference between two dissimilar images. The use of Siamese architecture is reasonable for similar image retrieval. Siamese architecture avoids network training requirements as part of its implementation principle.

Classical computing suffers from the loss of information in the process of computing. On the other hand, quantum circuits are able to provide reversible transformations of states. In other words, the unitary operator preserves the inner product space. Currently, researchers are showing interest to explore the applicability, scope, and prospect of quantum neural network in different fields. Parameterized quantum circuits (PQCs) are referred to as quantum neural network (QNN). It comprises three parts: encoding of classical data to quantum data, PQC, and measurement [1]. According to TensorFlow Quantum (TFQ) White Paper [2], TFQ is a quantum machine learning library, able to prototype quantum-classical machine learning models. TFQ supports the use of PQCs as Quantum Neural Networks (QNNs).

In this study, the proposed system deals with characteristic comparison and retrieval of exudate-affected retinal image patches. The system uses PQC implemented within the twin Siamese comparison structural foundation. It compares the query image patch and database image patches using tensor similarity computation. This technique can be utilized to implement a computer-aided diagnostic system leading to a decision regarding the manifestation of disease symptoms in retinal images. The system provides an opportunity to evaluate network performance in the quantum computing environment. It affords to cater a new skyline to the evolution of reversible computing in a popular healthcare research domain.

2 | RELATED WORK

Following are different research studies we studied during our work implementation. At the initial phase of research on content-based retrieval of retinal images, Ref. [3] contributed significantly. Ref. [3] retrieved images with a machine learning-based approach. Ref. [4] handled multimodal medical images for classification and content-based medical image retrieval with and without class prediction modelling. This study used a deep convolutional neural network. They claimed better accuracy for classification and better mean average precision for retrieval. Ref. [5] retrieved DR-affected retinal fundus images exploiting local binary patterns. Ref. [6] used Siamese CNN for similar work of DR-affected image retrieval. Ref. [7] retrieved similar images considering different pre-processing techniques and different features for vessels and exudates. In a very recent literature [8], retinal classification has experimented with quantum circuits in training of classical neural networks, and by designing and training quantum orthogonal neural networks. This work uses MNIST retinal dataset for image classification. They experimented with five qubits and nine qubits. They executed their experiments in the IBMQ processor as well as in simulators. They also reduced the image to four or 8 dimensions considering the current reach of quantum development. This work is an image classification work, not an image retrieval work.

Until now, the restriction of few qubits could not be overcome in the case of hybrid quantum classical model. This is due to gradient estimation complexity and the exponential dimension of Hilbert space or inner product space [9]. The probability of the gradient in a parameterized quantum circuit (PQC), towards any direction, is the function of the number of qubits involved and is non-zero to some fixed precision that is exponentially small. This problem requires further study. Ref. [10] discussed superposition and entanglement. These quantum phenomena can be used to solve problems of classical neural network learning. Quantum neural networks, when compared with equivalent classical neural networks, accomplish better performance and attain effective dimensions [11]. In Ref. [11], the authors utilized Fisher information spectrum of the barren plateaus to quantify the training capability of quantum models. They tried to deal with the vanishing gradient problem also. In Ref. [12], the authors designed a QNN that can be trained with supervised learning and is capable of representing classical or quantum labelled data. Unitary transformations are applied to qubits. These parameter-dependent transformations form the quantum circuit. Pauli operator is the predictor of QNN which is measured at the readout. This is the output of the binary predictor. Ref. [12] used a classical dataset comprising n bit string and the classes. The input quantum state is an n-bit computational basis. The circuit was implemented and labels were represented with Boolean function. A quantum feedforward neural network, capable of exercising universal quantum computations, is demonstrated in Ref. [13]. Here, the neurons are the quantum counterpart of classical neurons. The authors used fidelity as the cost function and proposed efficient training of QNN. It was claimed that the method was optimized faster and the memory requirements are less. According to Ref. [14], quantum convolutional neural network helps in evaluating the scope and prospect of CNN in quantum computing environment. It shows a horizon where a performance expansion is possible for an already existing learning model. The application of quantum CNN (QCNN) may open a new era of image recognition and proper research work is required on larger convolution kernels and inputs [15]. Quantum CNN is a circuit analogous to classical CNN in terms of non-linearity representation and pooling operation. Hybrid quantum-classical models enable the utilization of quantum computers to diversified application domains. Within this framework, parameterized quantum circuits can be regarded as machine learning models with remarkable expressive power [16].

Regarding classical data to quantum data conversion, in the Qubit Lattice model [17], every pixel is stored in a single qubit, and all pixel operations are changed into their quantum

counterpart operations on a single qubit. Thus, every quantum image is represented as a qubit matrix. Zhang et al. [18] also proposed a novel enhanced quantum representation (NEQR) for classical to quantum conversion of digital images. The application of NEQR can be observed in Ref. [19]. The experiment in Ref. [19] is carried out in both Cirq and Qiskit environments.

The role of quantum computing in the field of machine learning is tried to be explored by the Google AI Quantum team [20]. Quantum computers can be used for training a learning model using quantum environment. TensorFlow Quantum (TFQ) was released in early March, 2020 by Google along with the University of Waterloo and Volkswagen AG. Quantum machine learning (QML) is simulated with a python library named TensorFlow Quantum. TFQ simulates noisy intermediate-scale quantum (NISQ) devices that are available in the present era. These simulators run on classical computers allowing researchers to run and test qubit operations. Further, IBM Quantum Composer and IBM Quantum Lab provide access to cloud-based IBM quantum computing services to public and premium users on an online platform. IBM Qiskit provides open-source tools for handling quantum programs. An online open-source Qiskit textbook [21] is also maintained by IBM Qiskit community. Ref. [22] represented a discussion and review on simulation of quantum computation for classical neural network.

Currently, quantum applications are in a rapid developing phase. These applications utilize different quantum algorithms for higher accuracy and reduced time complexity compared to classical computing. Significant quantum computing benefit is likely to be observed in the healthcare sector also. Quantum computing does not merely provide an incremental speedup. Quantum computers may enable accurate diagnoses enabling precise treatments, as well as a better way to reflect cost beneficial model from the patient viewpoint. Quantum computing has the potential to sustainably improve medical image analysis and retrieval through image matching. These improvements would enhance image-aided diagnostics. Further, in references [11–15], authors experimented extensively on the training intricacies of quantum neural networks. In this work, we try to reap the results of removing this complex network training by implementing parameterized quantum circuit within Siamese architecture. Conversion of Cirq objects to TensorFlow string tensors enables to successfully compare and retrieve similar image patches. These may be considered as the motivations behind our work implementation.

In this study, we propose a quantum neural network implemented within Siamese architecture to evaluate the efficacy of this model for the affected image patch retrieval task. In a quantum neural network, entanglement gates are applied on input quantum states or qubits. Images are not directly resized and fed to QNN to avoid medically significant information loss. Instead 20 × 20 original image patches are taken and resized to 4 × 4 resolution. Otherwise, data cannot be handled with currently available quantum opportunities. This classical pre-processing certainly may reduce the system performance but we tried to benchmark such retrieval approach on the current quantum scenario and understand if quantum machine learning methods can be used as a better alternative to the classical approach in future. In classical Siamese neural network, elimination of weight adjustment and hidden layer manipulation are exploited to reduce the time, memory, and computational complexity of the task at hand. We propose a Siamese Quantum Neural Network which is capable of comparing two tensors representing the input patch and the database patch. Like its classical Siamese counterpart, weight updating and network training are avoided in this work. The intention is to extend the computation capability of classical Siamese neural network to the domain of quantum computing. QNN is evaluated on a simulation framework. In this way, it is tried to evaluate a different neurocomputing way for information processing.

The contribution of the work is the implementation of a quantum circuit within the Siamese paradigm in Cirq framework and evaluation of its applicability and efficiency in the research area of affected retinal fundus image retrieval through twin comparison of patch representations. Though retinal fundus image retrieval is a significantly explored research domain, yet the pertinence of applying either quantum computing itself or Siamese implementation of it has never been explored in the relevant field, as per our knowledge. Exudate-affected image patches are input to the retrieval system. Query patch and database patch are fed to two parallel and identical instances of the same PQC and the system retrieves similar images on the basis of Siamese comparison of circuit representation, converted to tensor. The outcome of our work is that the system performance is notable while retrieving affected image patches from the patch database. A different patch retrieval approach has been experimented in Qiskit framework also. In this approach, classical data is encoded using NEQR encoding algorithm and the probability distributions of measurement results of query patch and database patch are computed with Jeffreys distance. The experimental results are evaluated with widely used retrieval evaluation metrics such as mean average precision (MAP) and mean reciprocal rank (MRR). Managing ever growing visual data has now become quite critical for medical image retrieval systems. Evaluation of a large volume of medically significant data can be performed with quantum computation in an exponentially faster way though it requires further technological advancement. If the process would have been implemented in a quantum processor removing the restriction of handling few qubits, it may have yielded remarkable and optimistic results. Classical computation has the constraint of architecture that it is irreversible in nature. In quantum computation, quantum states are passed through quantum gates which are unitary operators, capable of producing reversible architecture. Unitary transformation is a bijection that preserves the inner products of tensors. Reversible computing is the future direction of energy and cost-effective computing. These possibilities may open up a new paradigm shift in the domain of classical computation. In Ref. [23], a detailed discussion regarding generalized reversible circuit design is available. Adiabatic logic avoids information loss and energy dissipation

in a logically reversible circuit. But the main challenge is to overcome qubit restriction and quantum hardware limitation in real life which is an ongoing process right now.

3 | PRELIMINARIES

3.1 | Diabetic Retinopathy symptoms

Retinopathy causes damages in the retina. In Diabetic Retinopathy (DR), retina gets damaged due to the development of Diabetes in patients. The most prevalent DR symptoms in the affected retina are presence of microaneurysm-haemorrhage (MA-HM) and exudates (EX). Abnormal widening or ballooning of vessel wall in DR-affected retinal images are microaneurysms. Weakened vessel walls are responsible for the development of this symptom. Blood filters out through these weak portions of blood vessels. Any fluid that leaks out in the inflammation area and gets deposited there is known as exudate.

3.2 | Content-based retrieval

In content-based retrieval, the visual content of the data helps in retrieving similar data samples. In an automated medical diagnosis system, a retrieval system can be utilized. Given an affected sample it helps in retrieving similar samples obtained from mass health screening procedures. Nowadays, CBIR is facing the need for managing ever-growing visual data.

3.3 | Quantum circuit implementation frameworks

Cirq was released by Google in the year 2020 [24]. Cirq is the open-source framework, capable of providing a quantum computing setup to experiment on NISQ quantum processors and quantum simulators. TensorFlow Quantum (TFQ) is a new open-source python library that affords quantum circuit simulator, parameterized quantum circuit (PQC). Cirq and Tensorflow have a common interface. Cirq provides the capability of circuit implementation with static and parameterized gates. Cirq and TFQ interface provides the simulation of noisy intermediate-scale quantum (NISQ) devices.

Qiskit is another open-source SDK provided by IBM [21]. Qiskit was released in the year 2017. Qiskit is used for working with quantum computer simulators and the IBM Q quantum processors. Aer simulator is a noisy quantum circuit simulator backend. The backend imitates the execution of a real device. The quantum circuit returns a dictionary of measurement outcomes.

3.4 | Siamese architecture

DNN requires a huge number of labelled samples for successful training. In the field of medical images, the difficulty to collect a huge number of labelled samples is still difficult. Here comes the concept of one shot learning which helps in learning and comparing through twin network. Twin network evaluates the reference sample and the test samples in parallel to compute the difference between them. The intermediate network features are compared to generate the similarity score. The less the difference between samples, the more is the similarity between them. This architecture avoids computationally exhaustive weight updating and training phase of the network.

3.5 | NEQR image representation

NEQR is one of the quantum image representation schemes [18]. Qubits are required to create a characteristic quantum circuit to represent a grayscale image. Two groups of qubits represent pixel values as well as pixel positions. Detailed illustration of NEQR is available in Ref. [25].

4 | IMPLEMENTATION REQUIREMENT

The experiments have been carried out with Intel Core i5 10,400F CPU @ 2.90 GHz with 6M Cache, upto 2.90 Ghz and 16 GB DDR4 RAM. Software versions used for work evaluation are as follows, Python 3.8.6, Tensorflow v1, Keras 2.3.1, Tensorflow.Quantum 0.4.0 and Cirq 0.9.1, qiskit 0.29.0, qiskit-aer 0.8.2.

5 | RETRIEVAL EVALUATION METRICS

The most commonly used image retrieval evaluation metrics [26] are mean average precision (MAP) and mean reciprocal rank (MRR).

We considered three predefined rank threshold values (K). For $K = 3$, 5, and 7, the percentage of relevant retrievals among top K retrievals indicates system precision. MAP is the mean of average precisions for different Ks.

$$MAP = 1/N \sum_{i=1}^{N} AP \tag{1}$$

In MRR, the first relevant rank value for retrieval is considered and the mean of reciprocal of rank values is computed over query sets.

$$MRR = 1/N \sum_{i=1}^{N} \frac{1}{rank_i} \tag{2}$$

where N is the number of elements in the query set and ranki is the rank of the first relevant retrieved sample in *i*th query.

6 | DATASET DESCRIPTION

E-ophtha [27] is a colour fundus image dataset. It comprises both healthy and Diabetic Retinopathy manifested images. Retinal images with different types of lesions (exudate and microaneurysm-haemorrhage) along with their ground truth versions annotated by ophthalmologists are there in the dataset. E-ophtha dataset contains two sub-databases. Microaneurysm-haemorrhage sub-database has 148 images with symptoms of micro aneurysms and small haemorrhages and 233 healthy images. Exudate sub-database has 47 images with symptoms of exudates and 35 healthy images. Three different resolutions, 2544 × 1696, 2048 × 1360, and 1440 × 960, are available in the dataset, for affected images, and two different resolutions, 2544 × 1696 and 1440 × 960, are available for healthy images. Ground truths are used as labelled samples.

7 | EXPERIMENTS

7.1 | Patch Extraction and Patch Database Formation

Retinal images are converted to the green channel and 20 × 20 overlapping patches are extracted from 47 exudate affected image samples. Further reduced patch sizes are not expected to encompass exudates properly. Affected and healthy patches are identified on the basis of a threshold number of affected pixels. We assumed that, in the case of affected patches, the number of affected pixels is greater than 100 whereas, in healthy patches, the number of affected pixels is less than 20. Figure 1 represents classical data preprocessing phase.

7.2 | Experiment in Google's cirq framework

The overview of the experiment in Google's Cirq framework is represented in Figure 2.

7.2.1 | Input to quantum circuit

The problem of handling more than a few qubits is still there in the field of quantum computing. Hence, 20 × 20 image patches are resized to 4 × 4. These 4 × 4 small patches are flattened and input to the circuit in the form of qubits. A rectangular lattice of 16 qubits is created from 16 intensity values available from the resized patch. Encoding classical image points to quantum datapoints is accomplished directly using the inbuilt mechanism of the Google Cirq environment. In qubit lattice model, one-to-one pixel-qubit mapping is maintained [17] to form the qubit lattice.

7.2.2 | PQC model creation using cirq

Quantum Neural networks are represented with parameterized quantum circuits (PQCs) which are defined with quantum gates. Sometimes, PQCs are quite efficient in producing significant inference. The classical data is pre-processed and fed to PQCs. At the output end as well, the classical processor observes the measurement values from the model output. Thus this model can be referred to as a quantum-classical model. TFQ loads quantum data as tensors. Cirq objects are converted to TensorFlow string tensors, with the tfq.convert_to_tensor function. The cirq.Circuit objects are parameterized by SymPy objects. These tensors are then converted to classical information via TFQ ops. Quantum states are produced as per the format of

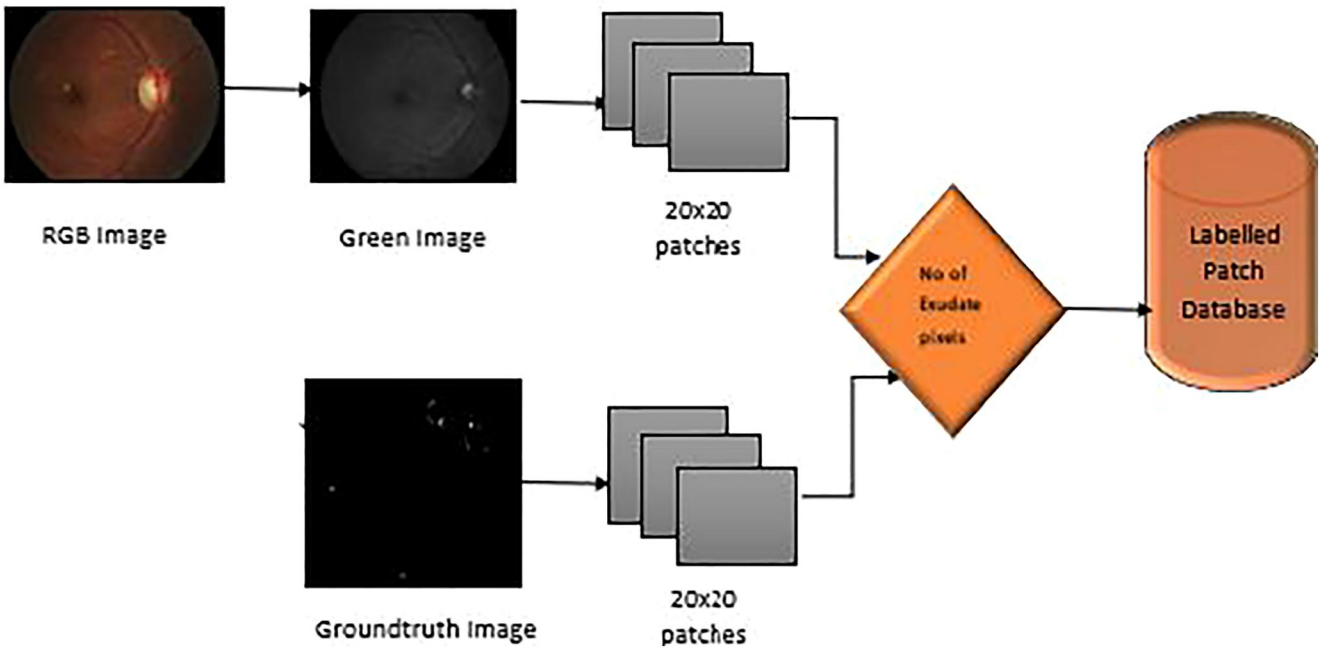

FIGURE 1 Patch extraction and patch database formation

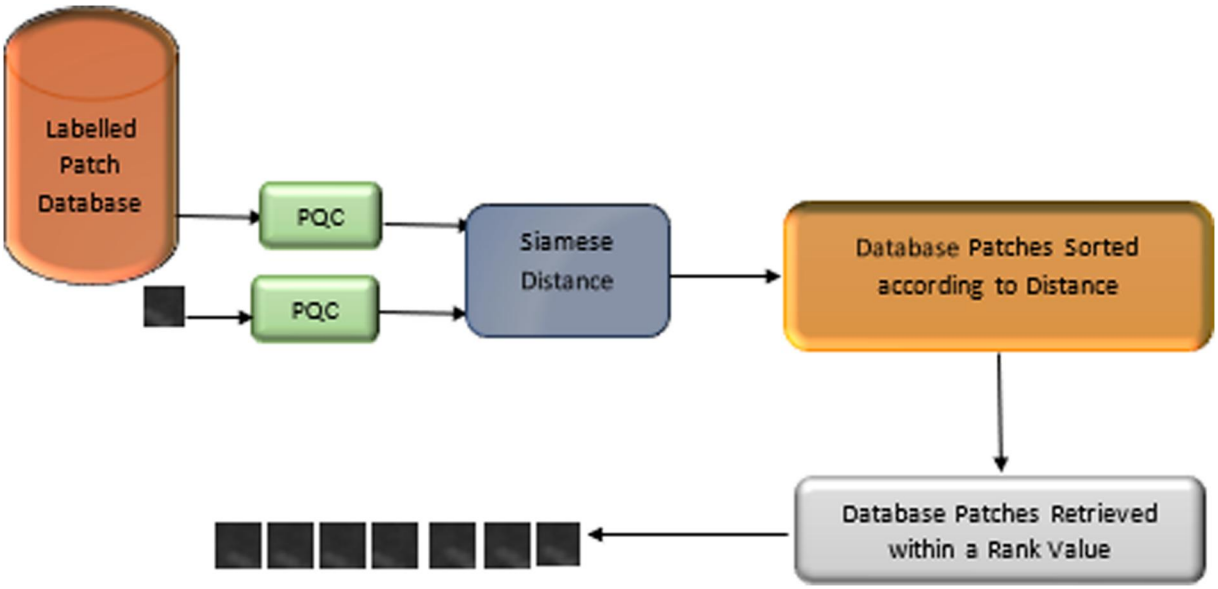

FIGURE 2 Experiment in Cirq environment. PQC, parameterized quantum circuit

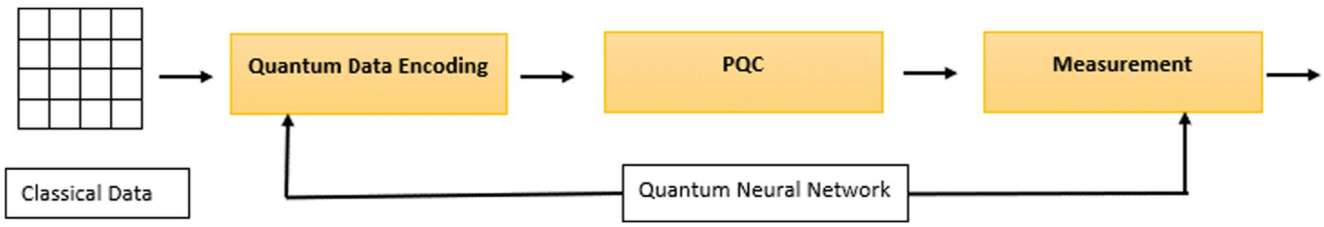

FIGURE 3 Block diagram of quantum neural network model. PQC, parameterized quantum circuit

FIGURE 4 Block diagram of quantum neural network model implementation in Cirq framework

PQCs and measurements are obtained. From measurement outcomes, predictions are computed. In this work, Cirq circuits are converted to TensorFlow Quantum circuits with defined data qubits and readout qubits. Circuit Layer Builder class is used to build model circuit. The model-circuit is enveloped in a tfq-keras model using Parameterized Quantum Circuit (PQC). A quantum circuit has been implemented where two qubit gates are used to connect each data input qubit and are directed to readout. Figures 3 and 4 show the block diagram of QNN model and the block diagram of QNN model implementation in Cirq framework, respectively. Summary of the parameterized quantum model is shown in Figure 5. The model has 32 model parameters. The detailed circuit diagram is present in Figure 10.

7.2.3 | Similarity score computation and retrieval in cirq

Input query patch and database patch are run through PQC in parallel. Input data is converted to rectangular grid qubits. PQC is applied over the tensors obtained by applying tfq package on the circuits. The absolute difference between the intermediate test patch tensor and database patch tensor from PQC is considered as the similarity score between these two patches. Thus, the whole database patches are compared with the query patch and sorted against absolute difference. Similar image patches are retrieved following sorted similarity score.

FIGURE 5 Parameterized quantum model

```
QNN Model Summary :
Model: "sequential"
_________________________________________________________________
Layer (type)                 Output Shape              Param #
=================================================================
pqc (PQC)                    (None, 1)                 32
=================================================================
Total params: 32
Trainable params: 32
Non-trainable params: 0
_________________________________________________________________
```

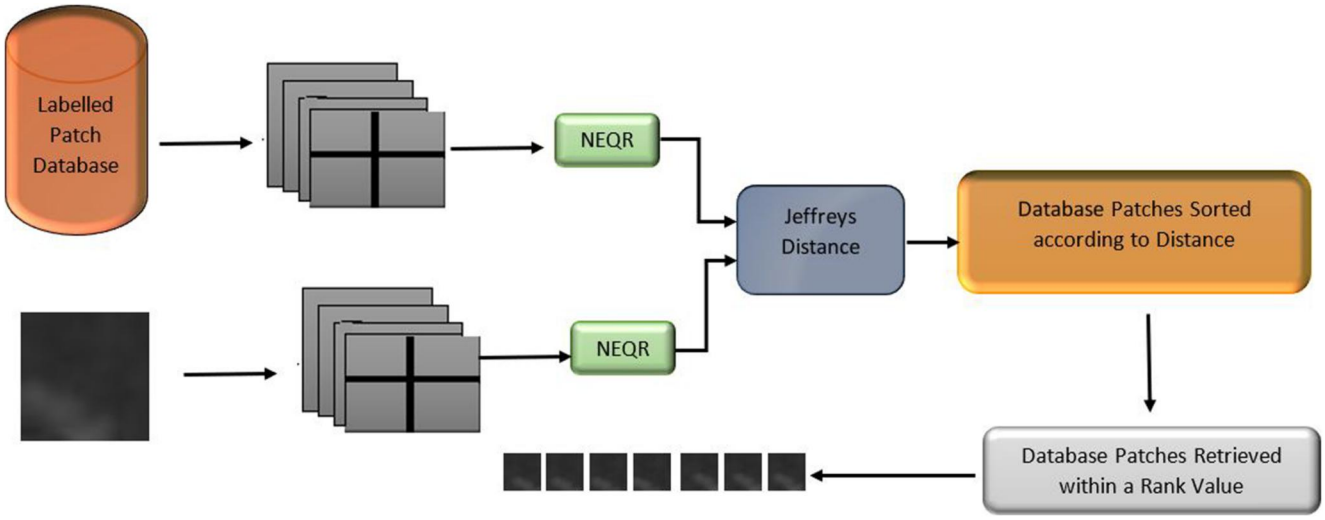

FIGURE 6 Experiment in Qiskit environment. NEQR, novel enhanced quantum representation

7.3 | Experiment in IBM's qiskit framework

The outline of the experiment in IBM's Qiskit framework is represented in Figure 6.

7.3.1 | Encoding pixels

In NEQR, pixel value encoding of a 2^n scale image requires n qubits. Thus to encode a grayscale image pixel in NEQR representation, eight qubits are required. If image size is 2×2, to represent each pixel position uniquely two qubits are required. So, to represent a 2×2 grayscale image, 10 qubits are required. To create the circuit, positional qubits are passed through Hadamard gates. To characterize grey pixels considering their binary representations, 1 bit along with its pixel position is encoded with CCX gate.

In general, a $2^n x 2^n$ resolution image can be represented in NEQR encoding scheme as a quantum state $|I\rangle$ [21] as

$$|I\rangle = \frac{1}{2^n} \sum_{Y=0}^{2^{2n-1}} \sum_{X=0}^{2^{2n-1}} |f(X,Y)\rangle |YX\rangle \sum_{Y=0}^{2^{2n-1}} \sum_{X=0}^{2^{2n-1}} \left| \otimes_{i=0}^{q-1} \right\rangle \left| C_{YX}^{i} |YX\right\rangle \tag{3}$$

So, for example, a 2×2 pixel image with four different pixel intensities, NEQR state will be represented as

$$\begin{aligned} |I\rangle = \left(\frac{1}{\sqrt{2}}\right) (& |00110011\rangle |00\rangle \\ & + |01100100\rangle |01\rangle |00000011\rangle |10\rangle \\ & + |01100000\rangle |11\rangle) \end{aligned} \tag{4}$$

where 00110011, 01100100, 00000011 and 01100000 are four different intensity values.

The detailed circuit diagram of NEQR encoding is given in Figure 13. Figure 7 shows the block diagram of NEQR circuit representation in Qiskit.

7.3.2 | Similarity score computation and retrieval in qiskit

The probability distribution of measurement results obtained out of quantum circuit representation of the grayscale image is used to find the distance between two patches. Jeffreys distance [28] indicates how similar those two probability distributions are. Jeffreys distance is defined as

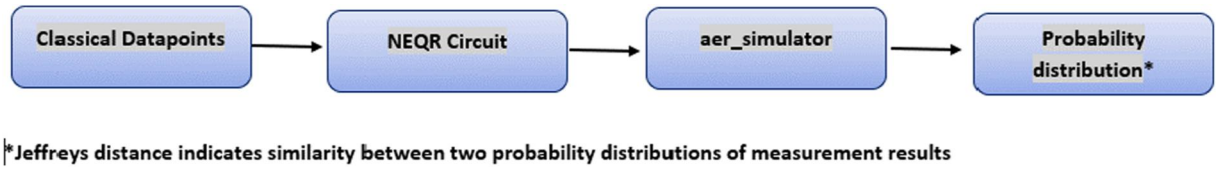

FIGURE 7 Block diagram of circuit comparison in Qiskit framework

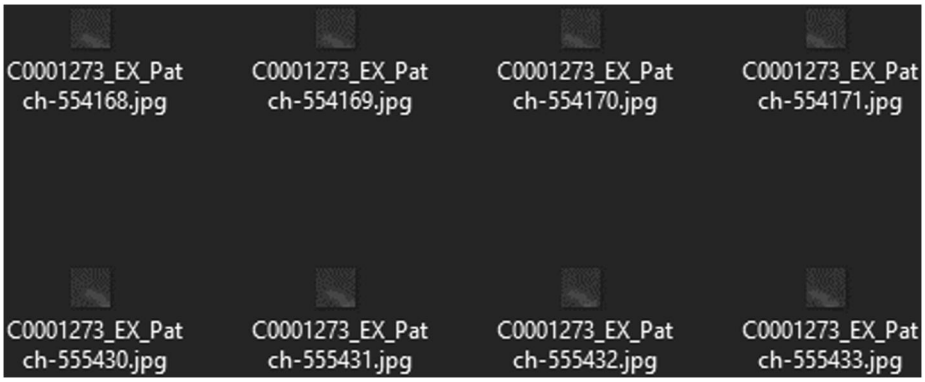

FIGURE 8 Some 20 × 20 affected patches

FIGURE 9 Some 20 × 20 healthy patches

$$K(P,Q) = \sum_{k=1}^{n} \left(\sqrt{p} - \sqrt{q}\right)^2 \tag{5}$$

where

$$\{P = (p1,\ p2,\ \ldots\ldots,\ pn) \mid 0 < pk < 1,\ \sum_{k=1}^{n} pk = 1\}$$

and $\{Q = (q1,\ q2,\ \ldots\ldots,\ qn) \mid 0 < qk < 1,\ \sum_{k=1}^{n} qk = 1\}$ are two discrete probability distributions.

This measure has many applications in pattern identification. Thus, the whole database patches are compared with the query patch and sorted against Jeffreys distance. Similar image patches are retrieved following sorted similarity scores.

8 | EXPERIMENTAL RESULTS

8.1 | Patch Extraction

Exudate-affected E-Ophtha images are converted to the green channel. From affected green channel images, 20 × 20 overlapping patches are extracted. These patches are considered normal patches if they contain the number of

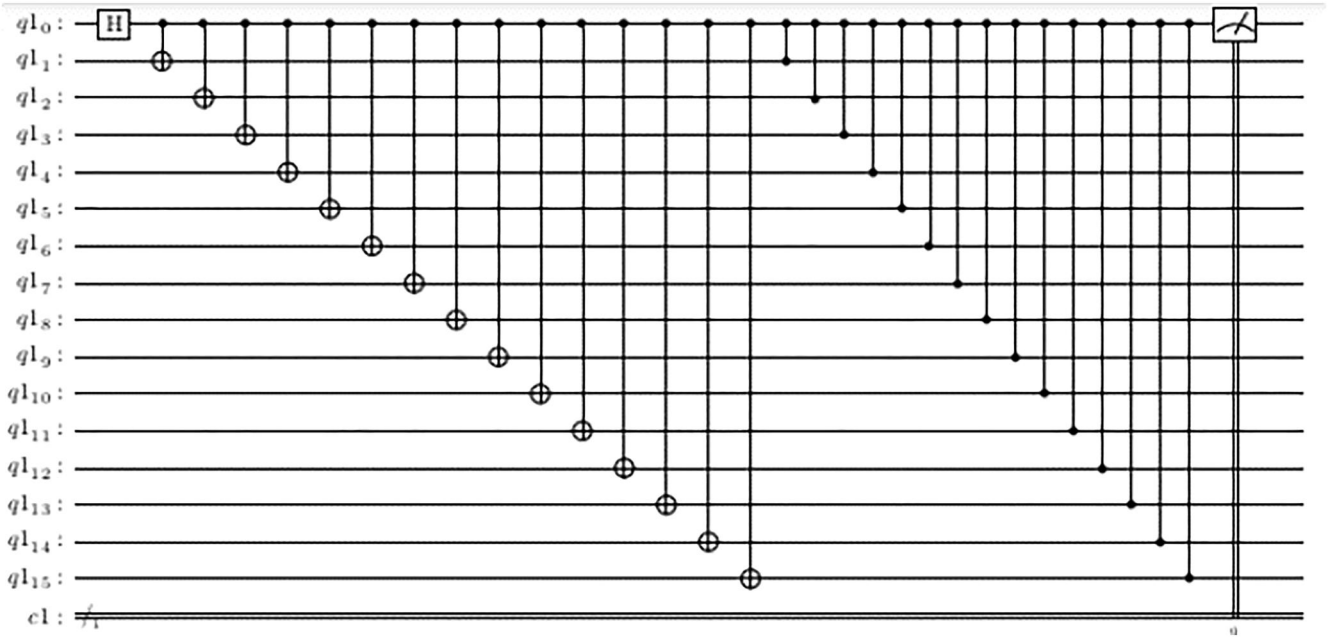

FIGURE 10 Cirq implementation-parameterized quantum circuit diagram

TABLE 1 Sample patch retrieval distances for query patch-C0001273_EX_Patch-561,745.jpg

Query patch- C0001273_EX_Patch-561745.jpg	
Retrieved patches	**Siamese tensor distance**
Positive -- C0001273_EX_Patch-608556.jpg	2.29E-05
Positive -- C0001273_EX_Patch-575646.jpg	3.31E-05
Positive -- C0001273_EX_Patch-608567.jpg	6.09E-05
Positive -- C0001273_EX_Patch-559272.jpg	6.82E-05
Positive -- C0001273_EX_Patch-581905.jpg	7.21E-05
Positive -- C0001273_EX_Patch-600978.jpg	7.33E-05
Positive -- C0001273_EX_Patch-571795.jpg	8.80E-05
Positive -- C0001273_EX_Patch-603510.jpg	0.000100628
Negative -- C0021833_EX_Patch-101052.jpg	0.000100628
Positive -- C0001273_EX_Patch-613608.jpg	0.000101958

TABLE 2 Sample patch retrieval distances for query patch-C0002369_EX_Patch-393,828.jpg

Query patch- C0002369_EX_Patch-393828.jpg results	
Retrieved patches	**Siamese tensor distance**
Positive -- C0001273_EX_Patch-568001.jpg	0
Positive -- C0001273_EX_Patch-566799.jpg	5.74E-08
Positive -- C0001273_EX_Patch-570526.jpg	5.86E-08
Positive -- C0001273_EX_Patch-564275.jpg	7.26E-08
Positive -- C0001273_EX_Patch-598333.jpg	1.93E-07
Positive -- C0002369_EX_Patch-397618.jpg	3.08E-07
Positive -- C0001273_EX_Patch-612218.jpg	4.63E-07
Positive -- C0001273_EX_Patch-570589.jpg	5.90E-07
Positive -- C0001273_EX_Patch-571788.jpg	5.90E-07
Positive -- C0001273_EX_Patch-570590.jpg	5.90E-07

affected pixels less than 20 and considered unhealthy if they contain the number of affected pixels greater than 100. Figures 8 and 9 show some affected patches and some unaffected patches.

8.2 | PQC model creation and retrieval in cirq

Two qubit gates are used to connect each data input qubit and directly forwarded to readout. 20 × 20 patches are resized to 4 × 4 patches, as quantum classical models are not able to manage more than few qubits until now [9]. The quantum model circuit has been implemented with 4 × 4 grid for data qubits and one readout qubit. Flattened images that is 16 classical pixel data points are converted by Cirq framework internally to 4 × 4 grid qubit. Google quantum AI defined cirq. GridQubit to label qubits by two numbers in a 4 × 4 grid of qubit lattice [17]. The circuit uses two-qubit gates which creates the connectivity between the data qubit and the readout qubit. The connectivity is implemented using consecutive Ising (XX) coupling gate and Ising (ZZ) coupling gate. The PQC diagram is displayed in Figure 10.

A total of 116,365 affected patches and 1,136,505 healthy patches have been extracted from 47 exudate-affected images available in E-ophtha dataset. The experimental patch database

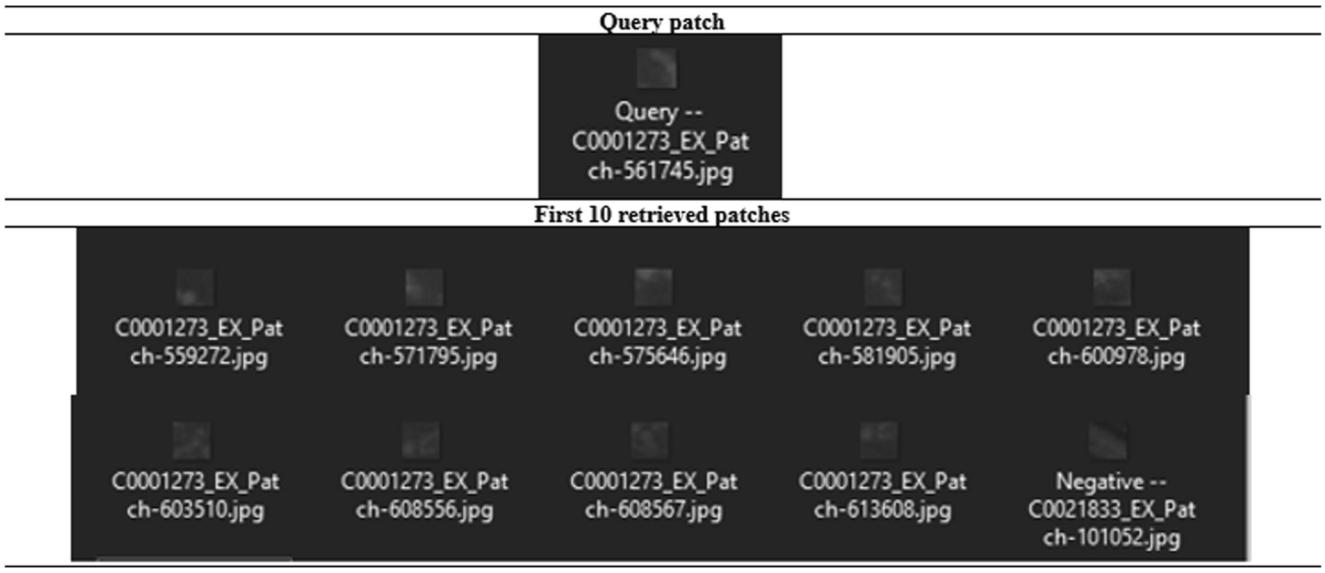

FIGURE 11 10 minimum distance patch retrieval visualization for query patch- C0001273_EX_Patch-561,745.jpg

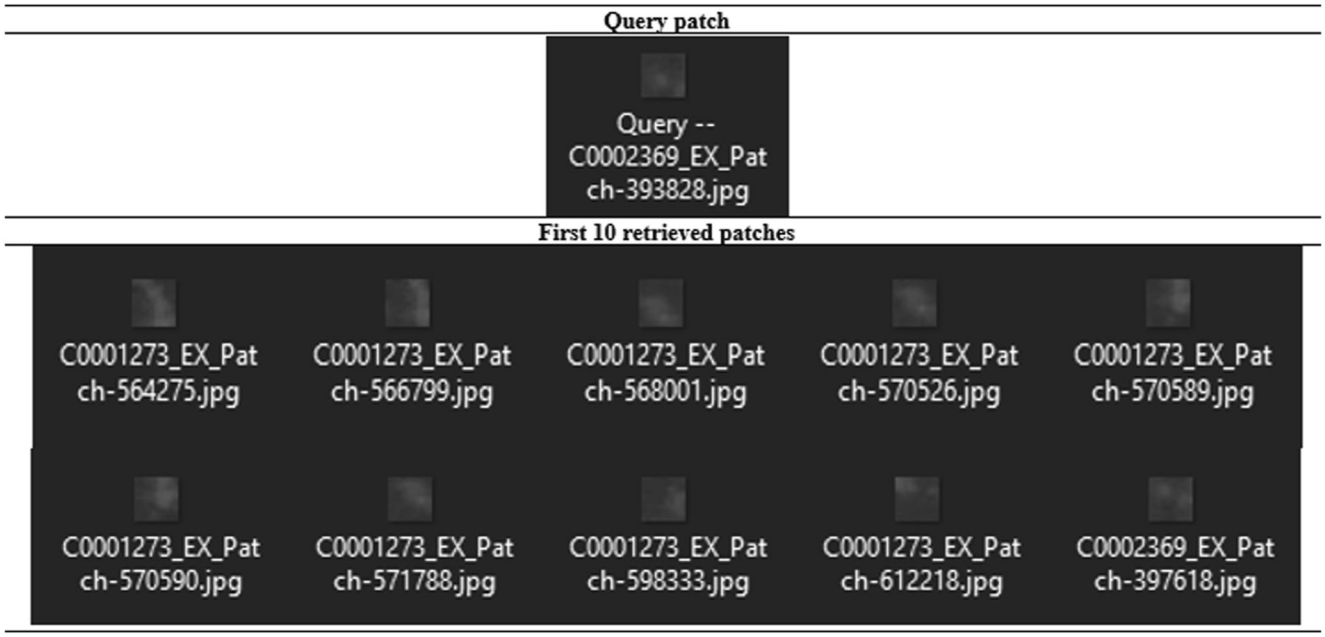

FIGURE 12 10 minimum distance patch retrieval visualization for query patch- C0002369_EX_Patch-393,828.jpg

TABLE 3 Mean average precision

	Precision			Metric
Sample query patch	$K = 3$	$K = 5$	$K = 10$	Average precision (AP)
C0001273_561745	100	100	90	96.67
C0001273_566737	100	100	100	100
C0001273_628776	100	100	100	100
C0002369_264807	100	100	100	100
C0002396_388536	100	100	100	100
Mean average precision (MAP)				99.334

TABLE 4 Mean reciprocal rank

	Reciprocal rank			Metric
Sample query patch	$K = 3$	$K = 5$	$K = 10$	Reciprocal rank (RR)
C0001273_561745	100	100	100	100
C0001273_566737	100	100	100	100
C0001273_628776	100	100	100	100
C0002369_264807	100	100	100	100
C0002396_388536	100	100	100	100
Mean reciprocal rank (MRR)				100

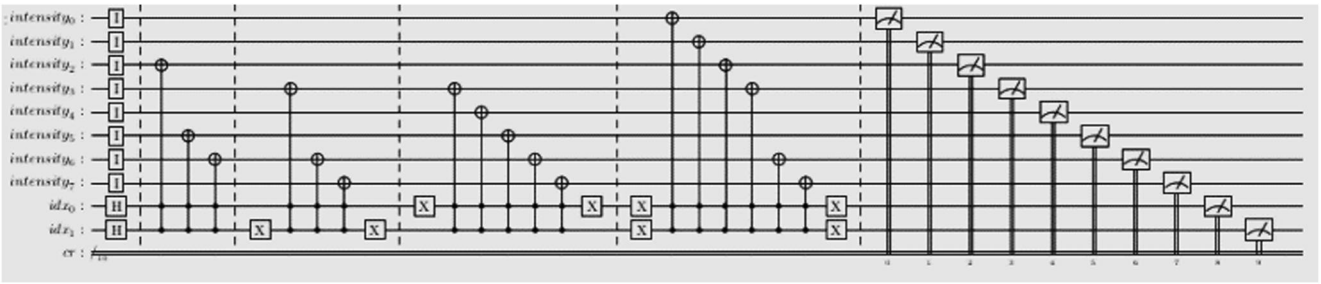

FIGURE 13 Qubit conversion circuit of a 2 × 2 quad of a 4 × 4 image patch

comprises 2475 affected patches and 2500 healthy patches whereas the query database consists of 250 exudate-affected patches. The outputs of the parameterized quantum circuit are converted to tensors and the absolute distance between these two extracted tensors is computed within the twin network architecture. Patches are sorted according to the distance and retrieved. Two sample patch retrieval results are given in Tables 1 and 2. Corresponding query and retrieved patch visualizations are obtained in Figures 11 and 12, respectively.

8.3 | Performance evaluation of cirq experiment

The retrieval performance has been evaluated with 250 exudate affected patches at rank $k = 3$, 5, and 10. The experimental mean average precision of this Siamese Quantum system is 98.1336%. The rank of the first retrieved similar sample is one in all the test cases. So mean reciprocal rank of the system is 100%. Average precisions and reciprocal ranks of some of the sample patches are referenced in Tables 3 and 4. Some more retrieval results are uploaded as Supporting Information.

8.4 | Pixel encoding and retrieval in qiskit

The image is subdivided into four quadrants of size 2 × 2. Grey valued pixels are represented with 8 bits. In Qiskit, the classical patch is converted to quantum patch applying NEQR algorithm. In this representation, eight qubits are required to encode grayscale value and two qubits are required to identify each position of a 2 × 2 image segment.

The similarity between two patches is computed considering the individual probability distribution of measurement results. The difference between two probability distributions has been computed using statistical distance metric – Jeffreys distance. Jeffreys distance is the measure of divergence between two probabilities. Figure 13 represents the Qubit conversion circuit of a 2 × 2 quad of a 4 × 4 image patch. Here, 1 bit along with its pixel position is encoded with controlled-controlled-not gate or Toffoli gate. Measurements are obtained accordingly.

8.5 | Performance evaluation of qiskit experiment

The retrieval performance of Qiskit experiment has been evaluated with 250 exudate-affected patches at rank $k = 3$, 5, and 10. Experimental mean average precision of this system is 52%. The mean reciprocal rank of the system is 71.36%. Average precisions and reciprocal ranks of some of the sample patches are referenced in Tables 5 and 6.

9 | DISCUSSION

Deep learning and convolutional neural network have been explored in the last decade for image similarity identification and retrieval. Deep network training requires a huge number of labelled training samples for successful learning. Further, this training phase is computationally heavy and consumes considerable training time. To cope with this hindrance, the Siamese network entered into the scenario where model training requirements are eliminated, instead image characteristics are compared in runtime inside the network. Thus, similar images or image patches are identified. If QNN can be utilized for image/image patch retrieval within Siamese architecture, QNN training will not be required to retrieve similar patches. On removing the shortcoming of using the restricted number of qubits, QNN is expected to provide fast and efficient information processing results in real life. The prospect of quantum learning has been explored from the viewpoint that the computation can be carried out without losing information that is, the computation can be reversed to recover the previous states. Reversible computing is the future trend for further improvement of generating energy-efficient computing algorithms. Quantum computers are able to compute matrix multiplication and tackle a large volume of data very fast as well.

In the application area of retinal image patch identification, the entire image is not resized to minimize medically significant information loss, instead, 20 × 20 overlapping patches are extracted from the image first. Patches of smaller sizes may not be able to represent exudates appropriately. Now, to overcome the limitations of quantum circuits which can still handle only few qubits, these patches are resized to a resolution of 4 × 4. Patches with different resolutions may also be used but the qubit capability of the device/simulator is to be considered

TABLE 5 Mean average precision

Sample query patch	Precision			Metric
	$K = 3$	$K = 5$	$K = 10$	Average precision (AP)
Positive--C0001273_607166	66.67	60	50	58.89
Positive--C0002369_418850	66.67	80	80	75.56
Positive--C0001273_605900	66.67	60	60	62.22
Negative--C0021833_100153	66.67	80	80	75.56
Negative--C0021833_100304	100	100	60	86.670
Mean average precision (MAP)				71.78

TABLE 6 Mean reciprocal rank

Sample query patch	Reciprocal rank			Metric
	$K = 3$	$K = 5$	$K = 10$	Reciprocal rank (RR)
Positive--C0001273_607166	50	50	50	50
Positive--C0002369_418850	50	50	50	50
Positive--C0001273_605900	100	100	100	100
Negative--C0021833_100153	100	100	100	100
Negative--C0021833_100304	100	100	100	100
Mean reciprocal rank (MRR)				80

TABLE 7 Comparison with other works

Method, year	Retrieval features	MAP	MRR	Category
Chandakkar et al., 2013 [3]	Lesion type/severity bag features	87.6%	–	ML based
Gajanan et al., 2017 [5]	Colour and LBP features	57.82%	–	Non-ML based
Chung et al., 2017 [6]	Deep features (3rd last layer)	62.09%	76.08%	DL based
	Deep features (2nd last layer)	63.69%	76.91%	DL based
	Deep features (SoftMax layer)	66.73%	77.45%	DL based
	Deep features (last layer)	64.92%	77.37%	DL based
Sukhia et al., 2019 [7]	Fused texture and shape features	79.47%	–	Non-ML based
Proposed method	Quantum features of image patches	98.1336%	100%	QNN based

Abbreviations: MAP, Mean Average Precision; MRR, Mean Reciprocal Rank; QNN, quantum neural network.

while creating the circuit. The research may reach from 50 to a few hundred qubits in the next few years which will empower the capability of quantum computing for sure.

In this work, two identical circuits are simultaneously input with images. Pair-wise distance measurement between the feature representations indicates whether the images are similar to each other. Intermediate network tensor encodings are extracted to compute the absolute difference between query patch and database patch. Siamese architecture removes the requirements of computation exhaustive network training. As per our knowledge, the QNN model never evaluated exploiting Siamese architecture in the field of content-based image retrieval. We are able to effectively capture the distance between two patches while the user input is an affected patch. QNN application may expose a new frontier in image identification, retrieval, and object detection.

Eyesight deterioration and other indicators of Diabetic Retinopathy arise late in the process of disease progression. Late diagnosis usually leads to an irreversible decline of vision which ultimately moves towards blindness. Early diagnosis and timely treatment slow down the disease progression remarkably. Quantum Neural Network has been achieved research interest recently. As per our knowledge, the contribution of QNN has not been evaluated in this field and to date, no papers are available on retinal image retrieval using QNN. Thus, providing any comparison table for previous retinal image retrieval performances using QNN is not possible. Hence, we provided a comparative performance table of similar retrieval work with

some non-machine learning-based, machine learning-based and deep learning-based approaches. In this work, QNN efficiency in the relevant field has been evaluated quantitatively with the most widely used retrieval evaluation metrics- MAP and MRR. As per the results obtained from experiments, the proposed QNN-based affected retinal patch retrieval system performs excellently in retrieving affected retinal patches. An affected patch is user input from a static database and the system will retrieve affected patches from the dataset, obtained from the mass Diabetic Retinopathy screening program. The results provide 98.1336% of MAP value and 100% MRR value, which is encouraging to observe the effectiveness of QNN involvement. Always the system is able to retrieve an affected patch as the most similar sample. We compare the performance of this work with state-of-art DR-affected retinal image retrieval works. Refs. [5, 7] are research references that retrieve DR-affected images following non-machine learning approaches whereas Ref. [3] retrieves DR-affected images exploiting traditional machine learning architectures. In Ref. [6], deep CNN architecture has been exploited by Yu-An Chung and Wei-Hung Weng. In this work, the effectiveness of retinal image retrieval is obtained considering layer wise deep features. They provided four different experimental results as shown in Table 7. They received the maximum MAP of 66.73% and maximum MRR of 77.45% for DR image retrieval considering SoftMax layer. These comparisons show better performance of QNN (Table 7), though our work represents a patch retrieval work considering the current limitation of quantum-classical network implementation.

10 | CONCLUSION

In this work, parameterized quantum circuit framework has been evaluated in the field of retinal image patch retrieval. The circuit has been implemented within the Siamese comparison paradigm in Google Cirq environment. A retrieval system has been implemented which is able to retrieve exudate-affected image patches by comparing Absolute distance between input exudate-affected patch and database patches. The proposed architecture received patch retrieval result Mean Average Precision of 98.1336% and a Mean Reciprocal Rank of 100%. Another retrieval approach has also been experimented in IBM Qiskit environment, where the probability distributions of explicitly encoded image pixel representations are compared for retrieval. Even though, the result is not impressive. Qiskit implementation of PQC is kept as the future scope of the work. We have not used any error correction algorithm. This may also be considered as another future scope of the work.

Until now, quantum classical model cannot be extended beyond few qubits, transformation is taking place which will lead to a more competent quantum technology developed in the future. Implementation and evaluation in a larger scale with a reversible quantum neural circuit is the future direction of this research. It is undoubtedly expected that quantum technologies will strive to successfully handle more and more qubits and eventually will move towards fault-tolerant computing. Minimizing quantum computation involvement through the use of error-correcting algorithm and allowing only the part of code which is difficult to evaluate on a classical computer, to execute in quantum processor, is the feasible pathway to reap the advantage of 'Quantum supremacy'.

CONFLICTS OF INTEREST

There is no conflict of interest.

PERMISSION TO REPRODUCE MATERIALS FROM OTHER SOURCES

None.

DATA AVAILABILITY STATEMENT

The manuscript has data associated with an online data repository (E-ophtha Dataset, A consortium of Institutes and Hospitals, France, Available: http://www.adcis.net/en/third-party/e-ophtha/, accessed on 02/06/2021).

ORCID

Mahua Nandy Pal https://orcid.org/0000-0002-9633-6718

REFERENCES

1. Alam, M., et al.: ICCAD Special Session paper: quantum-classical hybrid machine learning for image classification. arXiv preprint. arXiv: 2109.02862 (2021)
2. Broughton, M., et al.: TensorFlow Quantum: A Software Framework for Quantum Machine Learning. arXiv preprint. arXiv:2003.02989 (2020)
3. Chandakkar, P., Venkatesan, R., Li, B.: Retrieving clinically relevant diabetic retinopathy images using a multi-class multiple instance framework. In: Proceedings of SPIE Medical Imaging. Orlando (2013)
4. Qayyum, A., et al.: Medical image retrieval using deep convolutional neural network, Neurocomputing. 266. (2017)
5. Gajanan, M., et al.: Edgy salient local binary patterns in inter-plane relationship for image retrieval in Diabetic Retinopathy. Procedia. Comput. Sci. 115, 440–447 (2017)
6. Chung, Y.A., Weng, W.H.: December: Learning deep representations of medical images using siamese CNNs with application to content-based image retrieval. In: Proceedings of 31st Conference on Neural Information Processing Systems. NIPS, USA (2017)
7. Sukhia, K.N., Riaz, M.M., Ghafoor, A.: Content-based retinal image retrieval. IET Image Process. 13(9), 1525–1534 (2019)
8. Mathur, N., et al.: Medical Image Classification Via Quantum Neural Networks. arXiv preprint. arXiv:2109.01831 (2021)
9. McClean, J.R., et al.: Barren plateaus in quantum neural network training landscapes. Nat. Commun. 9(1), 1–6 (2018)
10. Schuld, M., Sinayskiy, I., Petruccione, F.: An introduction to quantum machine learning. Contemp. Phys. 56(2), 172–185 (2015)
11. Abbas, A., et al.: The Power of Quantum Neural Networks. arXiv preprint. arXiv:2011.00027 (2020)
12. Farhi, E., Neven, H.: Classification with Quantum Neural Networks on Near Term Processors. arXiv preprint. arXiv:1802.06002 (2018)
13. Beer, K., et al.: Training deep quantum neural networks. Nat. Commun. 11(1), 1–6 (2020)
14. Oh, S., Choi, J., Kim, J.: A Tutorial on Quantum Convolutional Neural Networks (QCNN). arXiv preprint. arXiv:2009.09423 (2020)
15. Kerenidis, I., Landman, J., Prakash, A.: Quantum Algorithms for Deep Convolutional Neural Networks. arXiv preprint. arXiv:1911.01117 (2019)
16. Benedetti, M., et al.: Parameterized quantum circuits as machine learning models. Quantum Sci. Technol. 4(4), 043001 (2019)
17. Venegas-Andraca, S.E., Bose, S.: Storing, processing and retrieving an image using quantum mechanics, Proceeding of the SPIE Conference Quantum Information and Computation. pp. 137–147. (2003)

18. Zhang, Y., et al.: NEQR: a novel enhanced quantum representation of digital images. Quantum Inf. Process. 12(8), 2833–2860 (2013)
19. Iqbal, B., Singh, H.: Identification of Desired Pixels in an Image Using Grover's Quantum Search Algorithm. arXiv preprint. arXiv:2107.03053 (2021)
20. Google AI Blog. Accessed on 29 December 2020. https://ai.googleblog.com/2018/12/exploring-quantum-neural-networks.html
21. Asfaw, A., et al.: Learn Quantum Computation Using Qiskit. (2020). http://community.qiskit.org/textbook
22. Mishra, N., et al.: Quantum Machine Learning: A Review and Current Status, Data Management, Analytics and Innovation. pp. 101–145 (2019)
23. Frank, M.P.: Foundations of generalized reversible computing. In: Phillips, I., Rahaman, H. (eds.) Reversible Computation: 9th International Conference. Lecture Notes in Computer Science, 10301, pp. 19–34. Springer, (2017). https://doi.org/10.1007/978-3-319-59936-6_2. https://link.springer.com/chapter/10.1007/978-3-319-59936-6_2
24. Google quantum AI: Textbook Algorithms in cirq. https://quantumai.google/cirq/tutorials/educators/textbook_algorithms
25. Yan, F., Venegas-Andraca, S.E.: Quantum Image Processing, pp. 19–48. Springer, Berlin (2020)
26. Manning, C.D., Raghavan, P., Schütze, H.: Introduction to information retrieval, Cambridge University Press, https://nlp.stanford.edu/IR-book/information-retrieval-book.html (2021). Accessed 14 Nov 2021
27. E-ophtha Dataset, A Consortium of Institutes and Hospitals. OPHDIAT© Tele-medical network, ANR-TECSAN-TELEOPHTA project funded by the French Research Agency (ANR). http://www.adcis.net/en/third-party/e-ophtha/ (2021). Accessed 02 June 2021
28. Chung, J.K., et al.: Measures of distance between probability distributions. J. Math. Analysis Appl. 138(1), 280–292 (1989)

SUPPORTING INFORMATION

Additional supporting information may be found in the online version of the article at the publisher's website.

How to cite this article: Nandy Pal, M., Banerjee, M., Sarkar, A.: Retrieval of exudate-affected retinal image patches using Siamese quantum classical neural network. IET Quant. Comm. 3(1), 85–98 (2022). https://doi.org/10.1049/qtc2.12026